




MicroRNA-146a Improved Acute Lung Injury Induced by hepatic Ischemia-reperfusion Injury by Inhibiting PRDX1

Dose-Response:
An International Journal
April-June 2023:1–9
© The Author(s) 2023
Article reuse guidelines:
sagepub.com/journals-permissions
DOI: 10.1177/15593258231169805
journals.sagepub.com/home/dos


Yiping Xu¹ , Yili Chen¹, Mengxia Yao¹, Yisheng You¹, Bin Nie¹, Meina Zeng¹, and Hui Jiang¹ 

Abstract

Hepatic ischemia-reperfusion injury (HIRI)-induced acute lung injury (ALI) is characterized by high incidence and poor prognosis. The regulatory role of microRNA-146a (miR-146a) in HIRI has been reported, but if miR-146a could affect the progression of HIRI-induced ALI has not been reported. The mice HIRI model was established by ligating left hepatic portal vein and hepatic artery for 60 minutes and then treating with reperfusion for 4 hours. Hypoxia-reoxygenation (HR) was performed to establish cell model. The binding site between miR-146a and Peroxidase I (PRDX1) was predicted and validated. The levels of inflammation factors and redox markers were detected with commercial kits. Significant lower expression of miR-146a and higher expression of PRDX1 in HIRI animal model were observed. miR-146a inhibited the liver injury after HIRI induction through targeting PRDX1. miR-146a inhibited the lung injury caused by HIRI via regulating PRDX1. The inhibition of cell apoptosis and inflammation factors by miR-146a were reversed by pcDNA-PRDX1. This research demonstrated that miR-146a improved ALI caused by HIRI by inhibiting apoptosis, inflammation, oxidative condition through targeting PRDX1. This study might provide a novel thought for the prevention and treatment of ALI caused by HIRI by regulating miR-146a/PRDX1 axis.

Keywords

miR-146a, PRDX1, acute lung injury, hypoxia-reoxygenation, hepatic ischemia-reperfusion injury

Introduction

Hepatic ischemia-reperfusion injury (HIRI) is also commonly observed in liver organ transplantation, partial hepatectomy, and hemorrhagic shock, and it is one of the important causes of postoperative complications.¹ Tissue damage caused by HIRI is the main cause of organ transplantation failure, liver dysfunction, and immune rejection.² HIRI is not only limited to the liver itself, but also endangers other organs and causes systemic diseases. Among them, acute lung injury (ALI) caused by HIRI is particularly prominent, with a high incidence, often resulting in poor prognosis and even death of patients.^{3,4} Solving the ALI caused by HIRI is the key to improve the prognosis and survival rate after liver transplantation. Therefore, it is very urgent and important to study the molecular mechanism of HIRI-induced ALI, and find new targets to improve the clinical treatments.

MicroRNAs (miRNAs) are a class of endogenously expressed non-coding single stranded RNA molecules with a

length of about 21–30 nucleotides, which can specifically bind to mRNAs and participate in post-transcriptional gene expression regulation.^{5,6} Usually, miRNAs combine with the 3' untranslated regions (3' UTR) of target genes to promote the degradation of target genes and participate in the regulation of various biological processes by inhibiting the expression of target genes.⁷ Studies indicated that the expression of multiple miRNAs was changed during HIRI. Non-coding RNAs

¹ Department of Anesthesiology, Clinical Oncology School of Fujian Medical University, Fujian Cancer Hospital, Fuzhou, Fujian Province, China

Received 26 October 2022; accepted 27 March 2023

Corresponding Author:

Hui Jiang, Department of Anesthesiology, Clinical Oncology School of Fujian Medical University, Fujian Cancer Hospital, No 420 Fuma Road, 350014, Fuzhou, Fujian Province, China.
Email: jianghui19850110@163.com



Creative Commons Non Commercial CC BY-NC: This article is distributed under the terms of the Creative Commons Attribution-NonCommercial 4.0 License (<https://creativecommons.org/licenses/by-nc/4.0/>) which permits non-commercial use, reproduction and distribution of the work without further permission provided the original work is attributed as specified on the SAGE

and Open Access pages (<https://us.sagepub.com/en-us/nam/open-access-at-sage>).

including long non-coding RNAs (lncRNAs) and miRNAs have been shown to influence I/R injury via regulating mitochondrial function, apoptotic and autophagic pathways, and signal transducers.^{8,9}

MicroRNA-146a (miR-146a) has been proved to be linked with the progression of several kinds of diseases. Conjugation of cerium oxide nanoparticles to miR-146a could improve diabetic wound healing by promoting angiogenesis and fibrotic processes,¹⁰ but decreasing inflammation, oxidative stress.^{11,12} The sustained release of miRNA146a-tagged cerium oxide nanoparticles could speed up diabetic wound healing time and significantly reduce inflammation.¹³ In addition, the conjugation of cerium oxide nanoparticles to miR-146a also inhibits pulmonary injury via reducing inflammation and oxidative stress, lowering collagen deposition.^{14,15} miR-146a was decreased in liver tissue and Kupffer cells during HIRI in mice.¹⁶ miR-146a played a protective role against HIRI,¹⁷ and inhibiting miR-146a expression in mice liver could aggravate HIRI.¹⁸ However, the regulation of miR-146a in ALI caused by HIRI has not been reported.

Previously, we applied bioinformatics to predict the target molecule of miR-146a. In TargetScan and miRDB databases, we found that Peroxidase 1 (PRDX1) may be the target molecule of miR-146a. PRDX1 plays an important role in ischemia-reperfusion injury, and PRDX1 is one of the members of the peroxidase family encoding antioxidant enzymes.¹⁹ PRDX1 is closely related to oxidative stress and is expressed in many different tissues and organs of the body. It is found that the expression level of PRDX1 in the lung is quite abundant,²⁰ suggesting that its function may be related to ALI caused by HIRI.

During HIRI, the mitochondrial structure is destroyed, and many apoptosis-related proteins are released into the cytoplasm due to the changes of mitochondrial membrane permeability, which directly mediates cell apoptosis.²¹ Bcl-2 can precisely change the permeability of mitochondria, form pores, and make the contents of mitochondria flow out.²² On the other hand, it can induce the opening of mitochondrial MPTP and promote the release of apoptosis-related proteins.²³ If miR-146a could regulate HIRI-induced ALI through affecting apoptosis has not been investigated.

In this study, HIRI-induced ALI animal model was established, and the cell model was established with hypoxia-reoxygenation (HR) method. We concluded that miR-146a could improve ALI induced by HIRI through inhibiting PRDX1. This research provides a novel thought for the prevention and treatment of HIRI-induced ALI.

Methods

Binding Site Prediction and Validation

According to the predicted results of binding site between miR-146a and PRDX1, the 3' UTR region of PRDX1 containing the binding site of miR-146a was cloned, and the

luciferase reporter plasmid PRDX1 3' UTR-reporter containing the 3' UTR of PRDX1 was constructed. A luciferase reporter plasmid (PRDX1 MUT reporter) containing PRDX1 3' UTR mutant was constructed. miR-146a overexpression lentiviral vector, PRDX1 reporter, PRDX1 MUT reporter were transfected into BEAS-2B cell line with lipo3000 liposome method. The luciferase activity was measured, and the regulatory effect of miR-146a on PRDX1 was validated.

Cell Culture and HR Model Establishment

BEAS-2B cell line was used in this study. The cells were incubated with DMEM high glucose medium at 37°C and 5% CO₂. After reaching 70% confluence, cell HR condition was established by incubating cells on the condition of 1% O₂, 94% N₂, and 5% CO₂ for 10 h, and reoxygenated for 4 h under normal condition. The cells in the group HR + miR-146a mimics were treated with miR-146a mimics (10 nM) for 24 h. The cells in the group HR + miR-146a mimics + pcDNA-PRDX1 were treated with miR-146a mimics (10 nM) and pcDNA-PRDX1 (10 nM) for 24 h. The cells in the group control and HR were treated with PBS for 24 h. Then, cells were used for different experiments.

Flow Cytometry

The cells were digested with trypsin, and cells were centrifuged at 2000 *g* for 10 min. The cells were suspended with binding buffer containing 5 μL propidium iodide and 5 μL Annexin V-FITC with cell apoptosis detection kit (#C1062S, Beyotime, China). After incubation for 15 min in the dark, cell apoptosis was detected with Novocyte cytometer.

Cell Transfection

The miR-146a mimic and pcDNA-PRDX1 were designed and constructed by GenePharma (Shanghai, China). Lipofectamine 3000 (Invitrogen, USA) was used for cell transfection according to the instruction. The concentrations of miR-146a mimic and pcDNA-PRDX1 were 20 nM. The RNA was extracted 24 h after transfection.

Establishment of HIRI Animal Model

All the experiments were approved by Ethical Committee of Affiliated Cancer Hospital of Fujian Medical University. C57BL/6J mice (20–30 g, Charles river, Beijing, China) were used in this study. Totally, 4 groups were set in this study with 10 animals in each group. The HIRI animal model was established as described previously,^{16,24} and modified by our team. The mice were anesthetized with xylazine (10 mg/kg) and ketamine (100 mg/kg) by intraperitoneal injection firstly. Under completely sterile conditions, the surgical mice were shaved and disinfected with

iodophor. Transabdominal midline laparotomy was performed, and the perihepatic ligaments were separated, the left hepatic hilum was dissected, and the left hepatic portal vein and hepatic artery were ligated with a small non-invasive artery clamp for 60 minutes before receiving reperfusion for 4 hours. The temperature of the animals was monitored during the operation. After anesthesia induction, buprenorphine (.1 mg/kg) was injected subcutaneously before skin incision for analgesia. In the sham group, only laparotomy was performed without other treatment. Then, the blood, lung tissues, and liver tissues were harvested after sacrificing mice. For the mice in the group HIRI + miR-146a mimics, miR-146a mimics (1×10^8 transfection units/mL) were injected through tail vein for three consecutive days before HIRI surgery. For the mice in the group HIRI + miR-146a mimics + pcDNA-PRDX1, miR-146a mimics (1×10^8 transfection units/mL) and pcDNA-PRDX1 (1×10^8 transfection units/mL) were injected through tail vein for three consecutive days before HIRI surgery. Same dose of normal saline was injected to the mice in the group sham and HIRI.

Western Blotting

The lung tissues, liver tissues, and cells were lysed first. The protein concentration was detected with BCA method. Equal amounts of protein (50 μ g) were loaded to SDS-PAGE gel electrophoresis (4% concentrated gel, 8–12% separation gel) for 2 h at 80 V. After electrophoresis, the gel was transferred to PVDF membrane (100 V, 100 mA, 2 h). The protein immobilized on the nitrocellulose filter membrane was pre-stained with Ponceau to confirm that the protein was indeed transferred to the membrane. 5% skim milk powder was used for blocking with TBST for 2 h and washed three times with TBS. Primary antibody was used to incubate membrane at 4°C overnight. TBS was used for washing 3 times. Horseradish peroxidase labeled Goat anti rabbit IgG (1:2000) was used to incubate membrane for 2 hours, and TBS was used for washing 3 times. Photographic analysis was performed with bio-image analysis system (Bio-Rad, Hercules, CA, USA).

Reverse Transcription Quantitative PCR

The lung and liver tissues were lysed, and RNA was extracted with Trizol reagent. 20 μ L RNA was dissolved with DEPC water, and RNA concentration was detected. Reverse transcription kit was used to reverse transcribe RNA into cDNA. The reaction system was set as follows: 95°C (30 s), 60°C (40 s), 70°C (70 s), with total cycles of 38. mRNA expression analysis was performed with $2^{-\Delta\Delta C_t}$ method. The primers were listed as follows: miR-146a: F: 5'-CAGTGCCTGTCGTGGAGT-3', R: 5'-GGGTGAGAACTGAATTCC-3';

PRDX1: F: 5'-TGCCAAGTGATTGGCGCTTCTG-3', R: 5'-AGCAATGGTGCCTTGGGATCT-3'.

Detection of Alanine Aminotransferase (ALT), Aspartate Aminotransferase (AST), Renin, Superoxide Dismutase (SOD), Glutathione (GSH), Malondialdehyde (MDA), TNF- α , IL-6, and IL-10

The serum levels of ALT, AST, and Renin were measured with related commercial kits purchased from Nanjing Jiancheng Bioengineering Institute according to instructions. The levels of SOD, GSH, MDA, TNF- α , IL-6, and IL-10 in lung tissues were measured with related commercial kits purchased from Nanjing Jiancheng Bioengineering Institute according to instructions.

Hematoxylin and Eosin (HE) Staining

The sections were dewaxed first, and incubated with hematoxylin for 5 min. After differentiation with 2% hydrochloric acid for 5 s, the sections were incubated with eosin for 1 min. After washing with water for 5 s, the sections were incubated with Xylene for 10 min. Neutral gum was used for sealing, and the slides were observed with a microscope (Carl Zeiss, Germany).

Tunel Staining

The sections were dewaxed and incubated with proteinase K working solution for 30 minutes. The sections were blocked with 3% hydrogen peroxide for 10 minutes and rinsed three times with PBS for 5 min each time. 50 μ L of TDT enzyme working solution was added to the sample, and the reaction was conducted at 37°C for 60 min in the dark. 50 μ L of streptavidin HRP working solution was added for incubation for 30 min. Then, the DAB (50 μ L) was used to incubate sections for 3 min. Hematoxylin staining was performed for 5 min, and dehydration with absolute ethanol for 7 min was conducted. Xylene was used for transparent for 7 min. The slides were observed with a microscope (Carl Zeiss, Germany).

Detection of IL-10, TNF- α , and IL-6

The levels of IL-10, TNF- α , and IL-6 were measured with related commercial kits purchased from Nanjing Jiancheng Bioengineering Institute according to instructions.

Measurement of wet and dry weight of lung tissue

The left lungs of mice were isolated, and wet weight was weighed. Then, the lung tissues were put in a micro oven at 65°C for 48 hours, and dry weight was weighed. The ratio between wet and dry weight was measured, and used to reflect the degree of pulmonary edema.

Statistical Analysis

Statistical analysis was performed with at least 3 repeated experiments. The data were presented as the mean \pm standard deviation. Data among different groups were analyzed with ANOVA. $P < .05$ was considered to be statistical difference.

Results

Significant Lower Expression of miR-146a and Higher Expression of PRDX1 in HIRI Animal Model Were Observed

The binding site between miR-146a and PRDX1 was predicted and identified first (Figure 1 (A)-(B)). The HIRI mice model was established and the overexpression vectors of miR-146a and PRDX1 were constructed. We found that the mRNA expression of miR-146a was markedly decreased in both lung and liver tissues after HIRI induction compared with group Sham (Figure 2A). However, after treatment with miR-146a mimics, the level of miR-146a was remarkably elevated, but pcDNA-PRDX1 presented no effects on expression of miR-146a (Figure 2A). In addition, the mRNA and protein expression of PRDX1 in lung and liver tissues were significantly increased in the group HIRI (Figure 2(B)-(D)), but overexpression of miR-146a significantly suppressed the level of PRDX1 (Figure 2(B)-(D)). Meanwhile, simultaneous administration with pcDNA-PRDX1 remarkably reversed the influence of miR-146a mimics, and elevated the expression of PRDX1. These finding indicated that miR-146a could negatively regulate PRDX1 in the HIRI animal model.

miR-146a Inhibited the Liver Injury After HIRI Induction Through Targeting PRDX1

After HIRI induction, the liver tissue structure was disordered, the cell space was increased, and the inflammatory cell infiltration was obviously observed compared with group HIRI (Figure 3A). However, overexpression of miR-146a markedly improved liver injury, but the improvement of liver tissue was reversed by pcDNA-PRDX1 (Figure 3A). In addition, the significant increase of ALT, AST, and Renin levels in the group HIRI were remarkably inhibited by miR-146a mimics. However, simultaneous treatment with pcDNA-PRDX1 greatly increased the levels of ALT, AST, and Renin compared with group HIRI + miR-146a mimics (Figure 3B).

miR-146a Inhibited the Lung Injury After HIRI Induction via Regulating PRDX1

In the sham group, the alveolar structure was clear without hemorrhage. In the group HIRI, the alveolar structure was destroyed, the alveolar septum was significantly widened, the capillaries in the alveolar wall were dilated, a large number of inflammatory cells were infiltrated, and large pieces of necrosis were seen in the lungs (Figure 4A). However, the pathological injury was greatly improved by miR-146a mimics, but overexpression of PRDX1 significantly reversed the influence of miR-146a and aggravated lung injury (Figure 4A). The apoptosis intensity in lung tissues was observed with Tunel staining. miR-146a mimics greatly suppressed the apoptosis levels in lung tissues compared with group HIRI, but the trend was reversed by pcDNA-PRDX1 (Figure 4B). Redox-related markers were

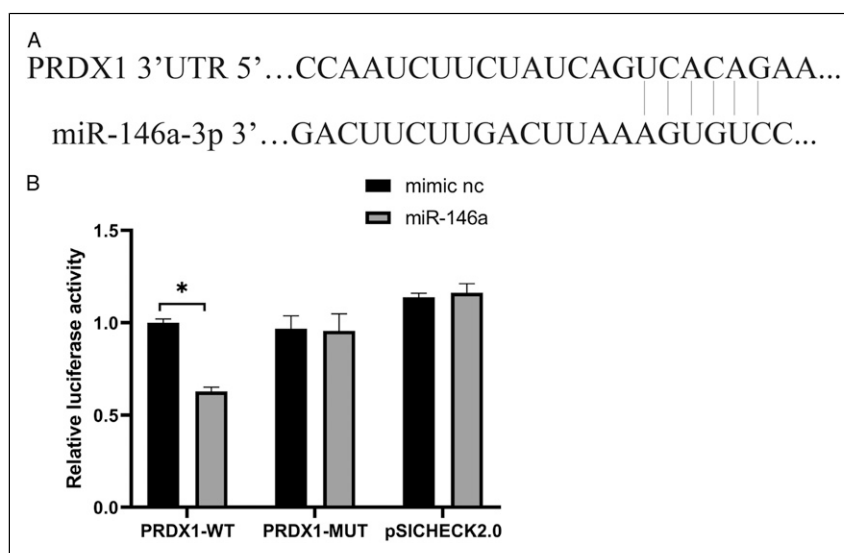


Figure 1. The binding site between miR-146a and PRDX1 was predicted and identified. (A) The binding site between miR-146a and PRDX1 was predicted through bioinformatics methods; (B) the binding site between miR-146a and PRDX1 was identified.

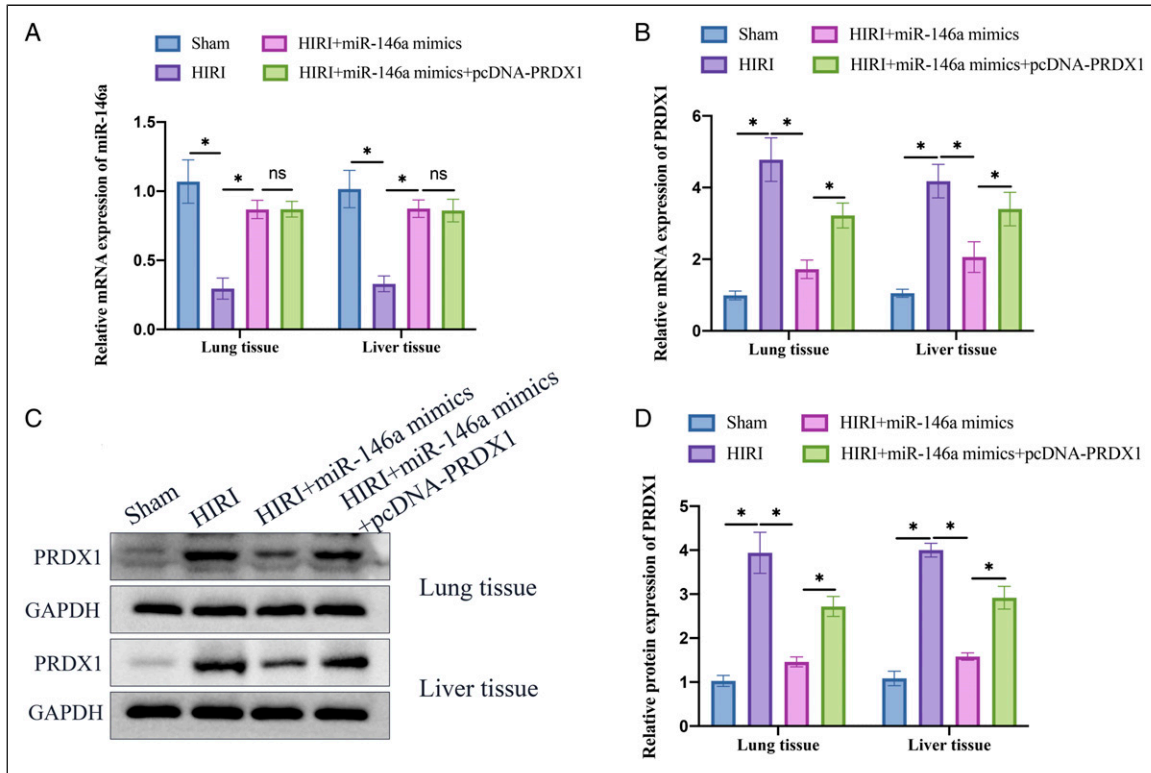


Figure 2. Significant lower expression of miR-146a and higher expression of PRDX1 in HIRI animal model were observed. (A) The mRNA level of miR-146a in both liver and lung tissues was measured after HIRI induction; (B) the mRNA level of PRDX1 in both liver and lung tissues was measured after HIRI induction; (C) the protein level of PRDX1 in both liver and lung tissues was measured after HIRI induction; (D) the protein level of PRDX1 was analyzed. * indicates $P < .05$.

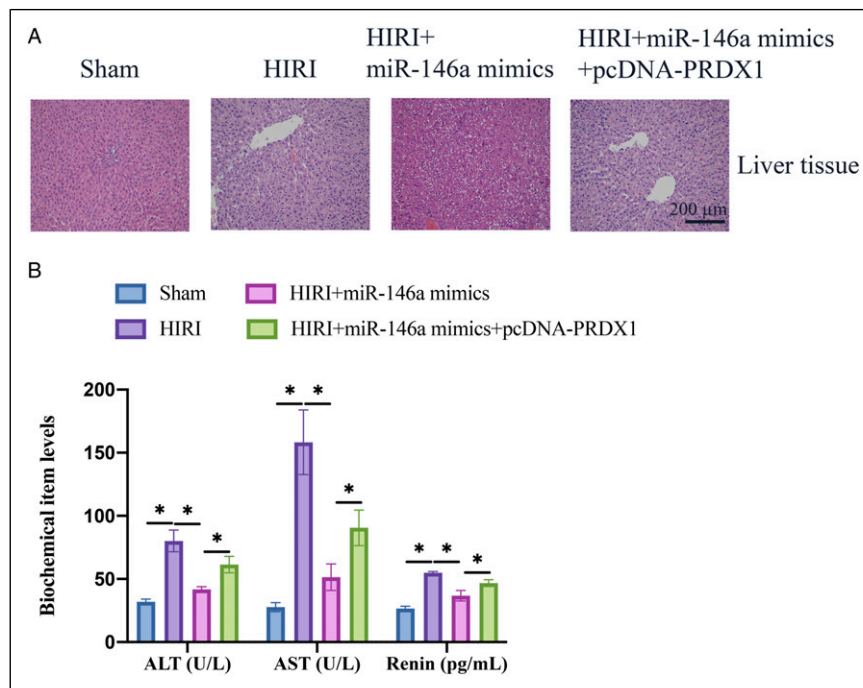


Figure 3. miR-146a inhibited the liver injury after HIRI induction through targeting PRDX1. (A) The liver tissue was observed through HE staining; (B) the levels of ALT, AST, and Renin were measured. * indicates $P < .05$.

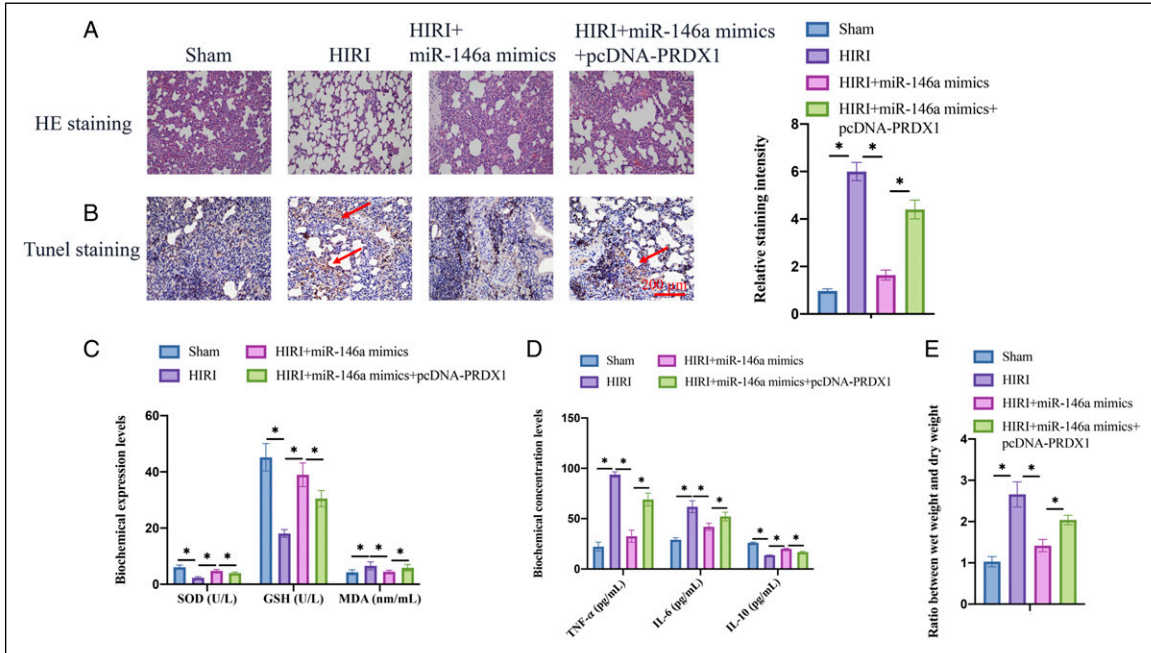


Figure 4. miR-146a inhibited the lung injury after HIRI induction via regulating PRDX1. (A) The lung tissue was observed through HE staining; (B) the apoptosis status in lung tissue was investigated with TUNEL staining; (C) the levels of SOD, GSH, MDA were detected; (D) the levels of TNF- α , IL-6, and IL-10 were detected; (E) the ratio between wet weight and dry weight was measured. * indicates $P < .05$.

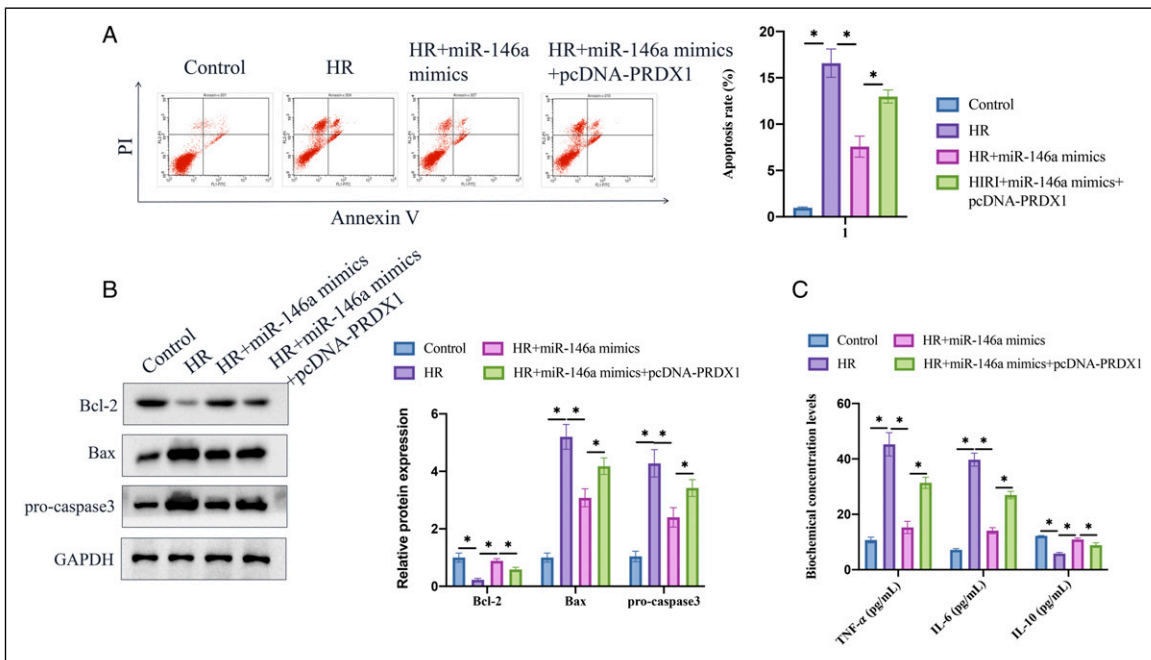


Figure 5. The inhibition of cell apoptosis and inflammation factors by miR-146a were reversed by pcDNA-PRDX1. (A) The cell apoptosis was measured with flow cytometry; (B) apoptosis-related proteins were measured with western blotting; (C) the inflammatory factors contents were measured. * suggests $P < .05$.

investigated in this study. We found that overexpression of miR-146a shown significant anti-oxidative effects by increasing SOD and GSH, but decreasing MDA (Figure 4C), and anti-inflammation effects by suppressing TNF- α and

IL-6, but promoting IL-10 (Figure 4D). However, overexpression of pcDNA-PRDX1 greatly reversed the influence of miR-146a on redox condition and inflammation factors expression. In addition, the decreased ratio between

wet weight and dry weight was promoted by pcDNA-PRDX1 (Figure 4E).

The Inhibition of Cell Apoptosis and Inflammation Factors by miR-146a Were Reversed by pcDNA-PRDX1

HR treated cell model was established first. We found that the cell apoptosis rate was remarkably increased after HR treatment compared to group control (Figure 5A). However, miR-146a mimics greatly inhibited cell apoptosis, but the influence of miR-146a mimics on cell apoptosis was markedly changed by pcDNA-PRDX1 (Figure 5A). Several apoptosis-related proteins were also measured. Overexpression of pcDNA-PRDX1 greatly reversed the influence of miR-146a mimics on apoptosis-related proteins expression by decreasing Bcl-2, increasing Bax and procaspase3 (Figure 5B). Meanwhile, the anti-inflammation effects of miR-146a mimics were also reversed by pcDNA-PRDX1 (Figure 5C).

Discussion

HIRI is a complex pathological process caused by multiple pathogenic factors, and the specific mechanism is not fully understood.²⁵ At present, the known pathogenesis of HIRI mainly includes the production of reactive oxygen species (ROS), the synthesis of inducible nitric oxide synthase (iNOS), the secretion of proinflammatory cytokines and chemokines, and the recruitment of immune cells and inflammatory cascade reaction.² During liver ischemia, Kupffer cells are activated and produce ROS in the early stage of reperfusion.²⁶ When the ischemia time is prolonged, xanthine oxidase and mitochondria in the cells can also produce ROS to aggravate liver dysfunction and cell damage during reperfusion.⁴ Kupffer cells and ROS activate macrophages and promote the recruitment of neutrophils, thereby aggravating the damage of blood vessels and parenchymal cells.²⁷

PRDX1 is a macrophage redox protein with multiple biological functions. The protein encoded by PRDX1 is a cytoplasmic protein, and PRDX1 was found to be a new injury-related molecule, and its expression was related to aggravating ALI and systemic inflammatory response.²⁰ PRDX1 could aggravate cerebral ischemia-reperfusion injury by activating inflammation and apoptosis.¹⁹ However, the role of PRDX1 in HIRI-induced ALI is unclear.

ROS can promote TNF- α , nitric oxide (NO), iNOS, chemotactic molecules and adhesion molecules, and further aggravate the inflammatory reaction.²⁸ TNF- α is mainly produced by Kupffer cells, and it is not only involved in inflammatory reaction, but also related to liver regeneration.²⁹ IL-10 can down regulate TNF- α during HIRI.³⁰ In the presented study, overexpression of miR-146a remarkably inhibited the increased levels of TNF- α , IL-6, but increased the concentration of IL-10 after HIRI induction

(Figure 4D). However, the influence of miR-146a was reversed by pcDNA-PRDX1.

A large amount of ROS production can induce oxidative stress injury, which is one of the pathological mechanisms leading to HIRI-induced ALI.³¹ The overproduction of ROS depends on Ca²⁺ transmission between endoplasmic reticulum and mitochondria, which not only directly causes oxidative damage of hepatocytes, but also leads to apoptosis.³² In addition, ROS can also cause lipid peroxidation, make the body produce a series of lipid peroxides, and affect the level of apoptosis-related markers and induce cell apoptosis.³³ In this study, the apoptosis status both *in vivo* and *in vitro* levels were also inhibited by treatment with miR-146a mimics. However, the suppression of apoptosis by miR-146a mimics was reversed by overexpressing PRDX1.

Conclusion

In the present study, we identified the binding site between miR-146a and PRDX1, and the negative regulation of miR-146a in PRDX1 was observed. The liver damage and ALI caused by HIRI was relieved by miR-146a mimics, but overexpression of PRDX1 markedly reverse the effect of miR-146a mimics on inflammatory factor expression, biochemical items concentration, and redox state. This study might provide novel thought for the prevention and treatment of HIRI-induced ALI via targeting miR-146a/PRDX1.

Author Contributions

HJ and YX conceived and designed the experiments; YX, YC, MY, YY, BN, and MZ performed the experiments; HJ, and YX wrote the paper. All authors read and approved the final manuscript.

Declaration of Conflicting Interests

The author(s) declared no potential conflicts of interest with respect to the research, authorship, and/or publication of this article.

Funding

The author(s) disclosed receipt of the following financial support for the research, authorship, and/or publication of this article: The study was supported by Startup Fund for scientific research, Fujian Medical University (2020QH1222).

Ethics Approval

The study has been approved by the Ethics Committee of Clinical Oncology School of Fujian Medical University, Fujian Cancer Hospital.

Informed Consent

All authors agree for the publication of this manuscript.

Data Availability

The datasets used in the current study are available from the corresponding author on reasonable request.

ORCID iDs

Hui Jiang  <https://orcid.org/0000-0002-2531-3113>

Yiping Xu  <https://orcid.org/0000-0002-1989-2534>

References

- Luo Y, Huang Z, Mou T, et al. SET8 mitigates hepatic ischemia/reperfusion injury in mice by suppressing MARK4/NLRP3 inflammasome pathway. *Life Sci.* May 15 2021;273:119286. doi:10.1016/j.lfs.2021.119286
- El-Sayed LA, Osama E, Mehesen MN, et al. Contribution of angiotensin II in hepatic ischemia/reperfusion induced lung injury: Acute versus chronic usage of captopril. *Pulm Pharmacol Ther.* 2020;60:101888. doi:10.1016/j.pupt.2020.101888
- Wang G, Li JY, Weng YQ, et al. Protective effect of ulinastatin combined with dexmedetomidine on lung injury after cold ischemia-reperfusion in rats. *Eur Rev Med Pharmacol Sci.* 2018; 22(17):5712-5718. doi:10.26355/eurrev_201809_15839
- Ge M, Chen C, Yao W, et al. Overexpression of Brg1 Alleviates Hepatic Ischemia/Reperfusion-Induced Acute Lung Injury through Antioxidative Stress Effects. *Oxid Med Cell Longev.* 2017;2017:8787392. doi:10.1155/2017/8787392
- Lauressergues D, Couzigou JM, Clemente HS, et al. Primary transcripts of microRNAs encode regulatory peptides. *Nature.* Apr 2 2015;520(7545):90-93. doi:10.1038/nature14346
- Cannell IG, Kong YW, Bushell M. How do microRNAs regulate gene expression? *Biochem Soc Trans.* 2008;36(Pt 6):1224-1231. doi:10.1042/BST0361224
- Li P, Chen Y, Juma CA, et al. Differential Inhibition of Target Gene Expression by Human microRNAs. *Cells.* Jul 30 2019; 8(8):791. doi:10.3390/cells8080791
- Ghafouri-Fard S, Shoorei H, Taheri M. Non-coding RNAs participate in the ischemia-reperfusion injury. *Biomed Pharmacother.* Sep. 2020;129:110419. doi:10.1016/j.biopha.2020.110419
- Ghafouri-Fard S, Shoorei H, Poornajaf Y, et al. NLRP3: Role in ischemia/reperfusion injuries. *Front Immunol.* 2022;13:926895. doi:10.3389/fimmu.2022.926895
- Sener G, Hilton SA, Osmond MJ, et al. Injectable, self-healable zwitterionic cryogels with sustained microRNA - cerium oxide nanoparticle release promote accelerated wound healing. *Acta Biomater.* Jan 1 2020;101:262-272. doi:10.1016/j.actbio.2019.11.014
- Dewberry LC, Niemiec SM, Hilton SA, et al. Cerium oxide nanoparticle conjugation to microRNA-146a mechanism of correction for impaired diabetic wound healing. *Nanomedicine.* 2022;40:102483. doi:10.1016/j.nano.2021.102483
- Niemiec SM, Louiselle AE, Hilton SA, et al. Nanosilk Increases the Strength of Diabetic Skin and Delivers CNP-miR146a to Improve Wound Healing. *Front Immunol.* 2020;11:590285. doi:10.3389/fimmu.2020.590285
- Zgheib C, Hilton SA, Dewberry LC, et al. Use of Cerium Oxide Nanoparticles Conjugated with MicroRNA-146a to Correct the Diabetic Wound Healing Impairment. *J Am Coll Surg.* 2019; 228(1):107-115. doi:10.1016/j.jamcollsurg.2018.09.017
- Niemiec SM, Hilton SA, Wallbank A, et al. Lung function improves after delayed treatment with CNP-miR146a following acute lung injury. *Nanomedicine.* 2022;40:102498. doi:10.1016/j.nano.2021.102498
- Niemiec SM, Hilton SA, Wallbank A, et al. Cerium oxide nanoparticle delivery of microRNA-146a for local treatment of acute lung injury. *Nanomedicine.* 2021;34:102388. doi:10.1016/j.nano.2021.102388
- Jiang W, Kong L, Ni Q, et al. miR-146a ameliorates liver ischemia/reperfusion injury by suppressing IRAK1 and TRAF6. *PLoS One.* 2014;9(7):e101530. doi:10.1371/journal.pone.0101530
- Chungen Y, Dongfang Z, Guoyuan X. MicroRNA-146a Protects Against Ischemia/Reperfusion Liver Injury Through Inhibition of Toll-like Receptor 4 Signaling Pathway in Rats. *Transplant Proc.* 2020;52(3):1007-1013. doi:10.1016/j.transproceed.2020.01.046
- Chen Q, Kong L, Xu X, Geng Q, Tang W, Jiang W. Down-regulation of microRNA-146a in the early stage of liver ischemia-reperfusion injury. *Transplant Proc.* 2013;45(2): 492-496. doi:10.1016/j.transproceed.2012.10.045
- Liu Q, Zhang Y. PRDX1 enhances cerebral ischemia-reperfusion injury through activation of TLR4-regulated inflammation and apoptosis. *Biochem Biophys Res Commun.* 2019;519(3):453-461. doi:10.1016/j.bbrc.2019.08.077
- Guo W, Liu X, Li J, et al. Prdx1 alleviates cardiomyocyte apoptosis through ROS-activated MAPK pathway during myocardial ischemia/reperfusion injury. *Int J Biol Macromol.* 2018;112:608-615. doi:10.1016/j.ijbiomac.2018.02.009
- Zaki AM, El-Tanbouly DM, Abdelsalam RM, Zaki HF. Plumbagin ameliorates hepatic ischemia-reperfusion injury in rats: Role of high mobility group box 1 in inflammation, oxidative stress and apoptosis. *Biomed Pharmacother.* Oct. 2018; 106:785-793. doi:10.1016/j.biopha.2018.07.004
- Li J, Wang F, Xia Y, et al. Astaxanthin Pretreatment Attenuates Hepatic Ischemia Reperfusion-Induced Apoptosis and Autophagy via the ROS/MAPK Pathway in Mice. *Mar Drugs.* May 27 2015;13(6):3368-3387. doi:10.3390/md13063368
- Tang SP, Mao XL, Chen YH, Yan LL, Ye LP, Li SW. Reactive Oxygen Species Induce Fatty Liver and Ischemia-Reperfusion Injury by Promoting Inflammation and Cell Death. *Front Immunol.* 2022;13:870239. doi:10.3389/fimmu.2022.870239
- Abe Y, Hines IN, Zibari G, et al. Mouse model of liver ischemia and reperfusion injury: method for studying reactive oxygen and nitrogen metabolites in vivo. *Free Radic Biol Med.* 1 2009; 46(1):1-7. doi:10.1016/j.freeradbiomed.2008.09.029
- Zhou L, Zhao D, An H, Zhang H, Jiang C, Yang B. Melatonin prevents lung injury induced by hepatic ischemia-reperfusion through anti-inflammatory and anti-apoptosis effects. *Int Immunopharmacol.* 2015;29(2):462-467. doi:10.1016/j.intimp.2015.10.012
- Zhang S, Cao Y, Xu B, et al. An antioxidant nanodrug protects against hepatic ischemia-reperfusion injury by attenuating oxidative stress and inflammation. *J Mater Chem B.* Apr 7 2022; 10:7563-7569. doi:10.1039/d1tb02689e

27. Konishi T, Lentsch AB. Hepatic Ischemia/Reperfusion: Mechanisms of Tissue Injury, Repair, and Regeneration. *Gene Expr.* 2017;17(4):277-287. doi:[10.3727/105221617X15042750874156](https://doi.org/10.3727/105221617X15042750874156)
28. Huang Y, Xu Q, Zhang J, et al. Prussian Blue Scavenger Ameliorates Hepatic Ischemia-Reperfusion Injury by Inhibiting Inflammation and Reducing Oxidative Stress. *Front Immunol.* 2022;13:891351. doi:[10.3389/fimmu.2022.891351](https://doi.org/10.3389/fimmu.2022.891351)
29. Ma H, Liu Y, Li Z, et al. Propofol Protects Against Hepatic Ischemia Reperfusion Injury via Inhibiting Bnip3-Mediated Oxidative Stress. *Inflammation.* 2021;44(4):1288-1301. doi:[10.1007/s10753-021-01416-z](https://doi.org/10.1007/s10753-021-01416-z)
30. Sahu A, Jeon J, Lee MS, Yang HS, Tae G. Nanozyme Impregnated Mesenchymal Stem Cells for Hepatic Ischemia-Reperfusion Injury Alleviation. *ACS Appl Mater Interfaces.* Jun 9 2021;13(22):25649-25662. doi:[10.1021/acsami.1c03027](https://doi.org/10.1021/acsami.1c03027)
31. Ghoneim MES, Abdallah DM, Shebl AM, El-Abhar HS. The interrupted cross-talk of inflammatory and oxidative stress trajectories signifies the effect of artesunate against hepatic ischemia/reperfusion-induced inflammasomopathy. *Toxicol Appl Pharmacol.* Dec 15 2020;409:115309. doi:[10.1016/j.taap.2020.115309](https://doi.org/10.1016/j.taap.2020.115309)
32. Li J, Li RJ, Lv GY, Liu HQ. The mechanisms and strategies to protect from hepatic ischemia-reperfusion injury. *Eur Rev Med Pharmacol Sci.* 2015;19(11):2036-2047.
33. Zhang S, Feng Z, Gao W, et al. Aucubin Attenuates Liver Ischemia-Reperfusion Injury by Inhibiting the HMGB1/TLR-4/NF- κ B Signaling Pathway, Oxidative Stress, and Apoptosis. *Front Pharmacol.* 2020;11:544124. doi:[10.3389/fphar.2020.544124](https://doi.org/10.3389/fphar.2020.544124)